The American Journal of Pathology, Vol. 171, No. 1, July 2007

DOI: 10.2353/ajpath.2007.060965

Vascular Biology, Atherosclerosis and Endothelium Biology

Human Immunodeficiency Virus Protease Inhibitor Ritonavir Inhibits Cholesterol Efflux from Human Macrophage-Derived Foam Cells

Xinwen Wang, Hong Mu, Hong Chai, Dan Liao, Qizhi Yao, and Changyi Chen

From the Molecular Surgeon Research Center, Division of Vascular Surgery and Endovascular Therapy, Michael E. DeBakey Department of Surgery, Baylor College of Medicine, Houston, Texas

Clinical use of human immunodeficiency virus protease inhibitors such as ritonavir may be associated with cardiovascular disease. The objective of this study was to determine the effects and molecular mechanisms of ritonavir on cholesterol efflux from human macrophage-derived foam cells, which is a critical factor of atherogenesis. Human THP-1 monocytes and peripheral blood mononuclear cells were preincubated with acetylated low-density lipoprotein and [^{3}H]cholesterol to form foam cells, which were then treated with apolipoprotein A-I for cholesterol efflux assay. A clinically relevant concentration of ritonavir (15 μmol/L) significantly reduced cholesterol efflux from THP-1 and peripheral blood mononuclear cells to apolipoprotein A-I by 30 and 29%, respectively, as compared with controls. In addition, ritonavir significantly decreased the expression of scavenger receptor B1 and caveolin-1, whereas it significantly increased superoxide anion production and activated extracellular signal-regulated kinase (ERK) 1/2 in macrophages. Mitochondrial membrane potential was significantly reduced, whereas NADPH oxidase subunits were increased in ritonavir-treated macrophages. Consequently, the antioxidant selenoL-methionine, the specific ERK1/2 inhibitor PD98059, or infection of a recombinant adenovirus encoding the dominant-negative form of ERK2 effectively blocked ritonavir-induced decrease of cholesterol efflux. Therefore, human immunodeficiency virus protease inhibitor ritonavir significantly inhibits cholesterol efflux from macrophages, which may be mediated by mitochondrial dysfunction, oxidative stress, ERK1/2 activation, and down-regulation of scavenger receptor B1 and caveolin-1. ***(Am J Pathol 2007, 171:304–314; DOI: 10.2353/ajpath.2007.060965)***

Human immunodeficiency virus (HIV) protease is an aspartic protease encoded by the *pol* gene and is required for posttranslational cleavage of *gag* and *gag-pol* precursor polyproteins into functional products needed for viral assembly.[1] Several HIV protease inhibitors (PIs) including ritonavir, amprenavir, indinavir, lopinavir, saquinavir, nelfinavir, and atazanavir have been developed to specifically inhibit HIV protease activities. These HIV PIs have been one of the most significant advances of the past decade in controlling HIV infection. However, long-term PI treatment may be associated with an increased risk of cardiovascular diseases such as atherosclerosis along with metabolic syndromes including systemic insulin resistance, dyslipidemia, and peripheral lipodystrophy.[1–3] It is not clear whether HIV PIs could affect macrophages in the vessels, an important mechanism of atherogenesis.

Cholesterol efflux is the process that removes excess cholesterol from tissues, including the arterial wall, thereby preventing the development of atherosclerosis.[4,5] Decreased cholesterol efflux from the arterial wall may potentially promote the progression of atherosclerosis. Cholesterol efflux can be mediated or regulated by several molecular pathways including ATP-binding membrane cassette transport protein A1 (ABCA1), G1 (ABCG1), scavenger receptor B1 (SR-B1), caveolins, and sterol 27-hydroxylase (CYP27A1).[6–10] Oxidative stress also affects cholesterol efflux in vascular smooth muscle cell-derived foam cells.[10,11] Oxidative stress has

Partially supported by the National Institutes of Health (research grants DE15543 and AT003094 to Q.Y.; and HL65916, HL72716, EB-002436, and HL083471 to C.C.).

Accepted for publication March 15, 2007.

Address reprint requests to Changyi (Johnny) Chen, M.D., Ph.D., Michael E. DeBakey, Department of Surgery, Baylor College of Medicine, One Baylor Plaza, Mail Stop: NAB-2010, Houston, TX 77030. E-mail: jchen@bcm.tmc.edu.

been implicated in cell injury, and a transient increase of reactive oxygen species (ROS) can result in the activation of various signaling pathways including the mitogen-activated protein kinases (MAPKs).

A major event in the progression of atherosclerosis is the differentiation of monocytes to macrophages that accumulate lipoprotein-derived cholesterol to form foam cells.[12] Using both *in vitro* and *in vivo* models, it has recently been shown that HIV PIs increase CD36-dependent cholesterol accumulation in macrophages independent of dyslipidemia.[13] Our recent investigations in both porcine arteries and human endothelial cells clearly demonstrated that PI ritonavir directly impaired vasomotor activities and endothelial monolayer permeability through the mechanism of oxidative stress,[14–18] indicating that PIs could directly cause the dysfunction or injury of vascular cells besides an indirect effect on vascular functions via HIV PI-induced abnormality of lipid and glucose metabolism.[19] Thus, we hypothesized that HIV PIs could have a direct effect on cholesterol efflux from macrophages, which may contribute to atherosclerosis progression.

The objective of this study was therefore to determine the effect of HIV PI ritonavir on cholesterol efflux from human macrophage-derived foam cells as well as to explore the possible molecular mechanisms. This study may advance our understanding on the mechanism of HIV PI-associated cardiovascular complications and suggest new strategies to control such clinical problems.

Materials and Methods

Chemicals and Reagents

Pure ritonavir powder was obtained from the AIDS Research and Reference Reagent Program, Division of AIDS, National Institute of Allergy and Infectious Diseases, National Institutes of Health, Bethesda, MD. Ritonavir was dissolved in dimethyl sulfoxide at the desired concentrations (7.5 to 30 μmol/L), and the final concentration of dimethyl sulfoxide in the experiments was adjusted to less than 0.1% (v/v), which was used in all controls. [1α,2α(*n*)-^{3}H]Cholesterol was purchased from Amersham (Piscataway, NJ) and human acetylated low-density lipoproteins (acLDL) and high-density lipoproteins (HDL) from Intracel (Frederick, MD). Rabbit polyclonal anti-SR-B1, -caveolin-1, -ABCA1, and -ABCG1 antibodies and mouse monoclonal anti-β-actin antibody were obtained from Norvus Biologicals (Littleton, CO). The oxidative fluorescent dye dihydroethidium (DHE) was obtained from Molecular Probes (Carlsbad, CA). Horseradish peroxidase-conjugated goat anti-rabbit IgG and anti-mouse IgG were purchased from Jackson ImmunoResearch (West Grove, PA). Bio-Plex phosphoprotein assays and Bio-Plex total target assays [specific for extracellular signal-regulated kinase (ERK)1/2, c-Jun NH_2-terminal kinase (JNK), and p38] were purchased from Bio-Rad (Hercules, CA). PD98059, a specific ERK1/2 inhibitor, was obtained from Calbiochem (San Diego, CA). Seleno-L-methionine (SeMet), ginsenoside Rb1, and apolipoprotein A-I (apoA-I) were obtained from Sigma (St. Louis, MO).

Cell Culture

Human THP-1 monocytes (human acute monocytic leukemia) were obtained from American Type Culture Collection (Manassas, VA) and cultured in RPMI 1640 medium containing 2 mmol/L glutamine, 20 IU/ml penicillin, 20 IU/ml streptomycin, 10 mmol/L HEPES, 1 mmol/L sodium pyruvate, 0.05 mmol/L 2-mercaptoethanol, and fetal bovine serum [10% (v/v)]. Cells were seeded onto 96-well plates at 2×10^5 cells per well and differentiated into macrophages by the addition of phorbol 12-myristate 13-acetate (100 ng/ml) for 5 days.

Fresh human blood samples were purchased from Gulf Coast Regional Blood Center (Houston, TX). Peripheral blood mononuclear cells (PBMCs) were purified by gradient centrifugation using Ficoll-Paque Plus (Amersham Biosciences, Uppsala, Sweden). PBMCs were seeded onto 96-well plates at 2×10^5 cells per well and cultured at 37°C in a 5% CO_2 atmosphere. The cells that adhered to the plate after 2 hours were used as monocytes and were allowed to differentiate into monocyte-derived macrophages for 5 days in RPMI 1640 medium containing 50 ng/ml M-CSF (macrophage colony-stimulating factor) and 1% fetal bovine serum, and the medium was refreshed every other day. PBMC-derived macrophages were used in the cholesterol efflux experiments.

acLDL Loading and Pretreatment

Macrophages were transformed into foam cells by incubation with acLDL (50 μg/ml) and [1α,2α(*n*)-^{3}H]cholesterol (1 μCi/ml) in the serum-free medium containing 1.5% bovine serum albumin for 48 hours. Radioisotope-containing medium was then removed, and cells were incubated for 24 hours in the medium containing bovine serum albumin and in the presence or absence of ritonavir (0 to 30 μmol/L), SeMet (50 μmol/L), ginsenoside Rb1 (10 μmol/L), or PD98059 (20 μmol/L).

Cholesterol Efflux

The macrophage-derived foam cells were then incubated in 100-μl serum-free medium with or without apoA-I (50 μg/ml) or HDL (100 μg/ml) for 24 hours. Cholesterol efflux from THP-1 macrophages was performed as previously described.[20] Cellular portion was lysed with 100 μl of 0.1 N NaOH. Samples (100 μl) of both supernatants and cell lysates were applied to UniFilter-96 plates (PerkinElmer, Boston, MA). After drying, samples were measured by TopCount-NXT (Packard, Downers Grove, IL) in the presence of 25 μl of MicroScint cocktail in each well. Fractional cholesterol efflux was calculated as [cpm(supernatants)/cpm(supernatants + cells)] $\times$ 100%.

Table 1. Genes and Sequences of PCR Primers

Gene	GenBank no.	Forward primer	Reverse primer
SR-B1	NM_005505	5′-ACCGCACCTTCCAGTTCCAG-3′	5′-ATCACCGCCGCACCCAAG-3′
Caveolin-1	NM_001753	5′-GACATCTCTACACCGTTCCCATCC-3′	5′-TCGTACACTTGCTTCTCGCTCAG-3′
Caveolin-2	NM_198212	5′-GCTGCGATGGGGCTGGAG-3′	5′-GCTGTGGTGGCTGTAGGAGTC-3′
CYP27A-1	NM_000784	5′-CACGACATCCAACACGCTGAC-3′	5′-GCACCACACCCACCACTTCC-3′
ABCA1	NM_005502	5′-GTCCTCTTTCCCGCATTATCTGG-3′	5′-AGTTCCTGGAAGGTCTTGTTCAC-3′
ABCG1	NM_004915	5′-CGGAGCCCAAGTCGGTGTG-3′	5′-TTTCAGATGTCCATTCAGCAGGTC-3′
p22phox	BT006861	5′-CAGATCGAGTGGGCCATGTG-3′	5′-AAAGTACCACTGGGTGAAGCG-3′
p40phox	NM_000631	5′-GCCAGACTGGAGAGAAGCAG-3′	5′-GTTCACCTCTCACTTCCTCCAG-3′
p47phox	AF330627	5′-TGGATCCCAGCATCCTTCCTC-3′	5′-CCTTGATGGCGACGTATGGC-3′
p67phox	AF527950	5′-TGTTTCGACCAAATGAGAGACAAG-3′	5′-GCAAACCCAGAGAAACTGTCTTG-3′
SOD1	NM_000454	5′-ATGACTTGGGCAAAGGTGGAAATG-3′	5′-GTTAAGGGGCCTCAGACTACATCC-3′
Catalase	NM_001752	5′-GCGGAGATTCAACACTGCCAATG-3′	5′-CTGTTCCTCATTCAGCACGTTCAC-3′
GPX1	NM_000581	5′-CGAGGGAGGAACACCTGATCTTAC-3′	5′-GGGAAACTCGCCTTGGTCTGG-3′
β-Actin	BC013835	5′-CTGGAACGGTGAAGGTGACA-3′	5′-AAGGGACTTCCTGTAACAATGCA-3′

ABCA1 (G1), ATP-binding membrane cassette transport protein A1 (G1); GPX, glutathione peroxidase; SR-B1, scavenger receptor B1; SOD, superoxide dismutase.

Intracellular Cholesterol Measurement

Cellular cholesterol levels were analyzed at the end of the efflux phase. Briefly, macrophages were washed with Dulbecco's phosphate-buffered saline. Their lipid content was extracted by addition of hexane/isopropanol [3:2 (v/v), 1 hour]. Cellular cholesterol levels were determined using cholesterol assay kit (Wako, Richmond, VA). Cellular proteins were determined with Pierce (Rockford, IL) protein assay against bovine serum albumin standard.

Cell Infection of Recombinant Adenoviruses Encoding Dominant-Negative Form of ERK2

At the end of acLDL loading stage, monocyte-derived macrophages were infected with recombinant adenoviruses encoding the dominant-negative form of human ERK2 (Cell Biolabs, San Diego, CA) or green fluorescent protein (GFP) at 200 multiplicity of infection followed by a 72-hour incubation at 37°C in a CO_2 incubator. More than 90% cells were infected, which was confirmed by evaluating GFP infection under the fluorescence microscope. Thereafter, the cells were pretreated with 15 μmol/L ritonavir followed by cholesterol efflux as mentioned above.

Real-Time Reverse Transcriptase-Polymerase Chain Reaction (RT-PCR)

Macrophage-derived foam cells were treated with ritonavir for 24 hours. Total cellular RNA was then extracted using a RNAqueous-4PCR kit (Ambion, Austin, TX). Primers for ABCA1, ABCG1, SR-B1, caveolin, CYP27A1, and several enzymes related to superoxide anion production including NADPH oxidase subunits $p22^{phox}$, $p40^{phox}$, $p47^{phox}$, and $p67^{phox}$, were designed via the Beacon Designer 2.1 software (Bio-Rad) (Table 1). The iQ SYBR Green supermix kit and iCycler iQ real-time PCR detection system (Bio-Rad) were used in real-time PCR. A housekeeping gene, β-actin, was included for internal control and comparison. Relative mRNA levels of genes of interest were presented as $2^{[Ct(\beta\text{-actin}) - Ct(\text{gene of interest})]}$ as previously described.[21]

Western Blot Analysis

Cell lysates were prepared at the end of the efflux phase from foam cells. Proteins were extracted with cell lysis buffer (Cell Signaling Technology, Inc., Danvers, MA). Equal amount of total proteins (50 μg) were loaded onto 10% sodium dodecyl sulfate-polyacrylamide gel electrophoresis, fractionated by electrophoresis, and transferred to polyvinylidene difluoride membranes. The membrane was incubated with the primary antibody at 4°C overnight. Dilutions of 1:2000 for SR-B1, 1:1000 for caveolin-1, 1:500 for ABCA1, and 1:1000 for ABCG1 were used. Bands were visualized with ECL Plus chemiluminescent substrate (Amersham Biosciences). Densitometric measurement was performed to quantify the relative expression of target proteins versus β-actin (AlphaEaseFC software; Alpha Innotech, San Leandro, CA).

Superoxide Anion Analysis by Flow Cytometry

The oxidative fluorescent dye DHE was used to evaluate the production of superoxide anion in the cells. DHE is freely permeable to cells. In the presence of superoxide anion, DHE is oxidized to ethidium bromide with red fluorescence, and it is trapped by intercalating with the DNA. Ethidium bromide is excited at 488 nm with an emission spectrum of 610 nm. Thus, the amount of ethidium bromide detected by fluorescence measurement instruments such as flow cytometer is well correlated to the level of cellular superoxide anion. Macrophage-derived foam cells were treated with or without ritonavir or SeMet in the 12-well plates for 24 hours. Cells were incubated with 0.5 ml of DHE (10

μmol/L) for 20 minutes at room temperature. Superoxide anion in the cells was analyzed by FACSCalibur flow cytometry (Becton Dickinson, San Jose, CA).

Assessment of Mitochondrial Membrane Potential (Δψm)

Δψm was assessed by using flow cytometry analysis of cells stained with 5,5′,6,6′-tetrachloro-1,1′,3,3′-tetraethylbenzimidazole-carbocyanide iodine (JC-1, MitoScreen kit; BD Biosciences). Mitochondria with a normal Δψm concentrate JC-1 into aggregates (red fluorescence). Cells (5×10^5) were incubated with 10 μg/ml JC-1 for 15 minutes at 37°C and analyzed by FACSCalibur flow cytometry.

Measurement of ATP Levels

ATP levels were measured with an ATPLite kit (Perkin-Elmer, Wellesley, MA) following the manufacturer's instructions. In brief, cells were seeded on 96-well plates (10,000 cells/well) and cultured with or without 15 μmol/L ritonavir for 24 hours. The lysis solution and substrate solution were added to each well of the plate. The luminescence was measured by TopCount-NXT.

Bio-Plex Immunoassay

Macrophage-derived foam cells were treated with 15 μmol/L ritonavir for 0, 5, 10, 20, 30, 60, 90, and 120 minutes. Cell lysates for the MAPK immunoassay were prepared using Bio-Plex phosphoprotein assay and Bio-Plex total target assay kits, in which 25 μg of proteins were used for MAPK measurement. The kits were applied on a Luminex multiplex system (Bio-Rad) following the manufacturer's instructions, which can detect the amount of phosphorylated and total ERK1/2, p38, and JNK in a small amount of cell lysates. Results were presented as the ratio of phosphorylated and total target proteins.

Statistical Analysis

All data are presented as the mean ± SEM. Sample size (n) in this study represents the numbers of independent sets (wells) of cells (multiple samples) from each experiment. Each major experiment was performed at least two times or more. Intergroup differences were analyzed using one-way analysis of variance for comparison of three or more groups. Student's t-test was used for comparison between two groups. A P value <0.05 was considered significant.

Results

Ritonavir Inhibits Cholesterol Efflux from Macrophage-Derived Foam Cells

We first tested the effect of ritonavir on cholesterol efflux from foam cells by measuring [^{3}H]cholesterol with a TopCount system. Macrophage-derived foam cells were treated with several concentrations (from 0 to 30 μmol/L) of ritonavir, and cholesterol efflux was initiated by the

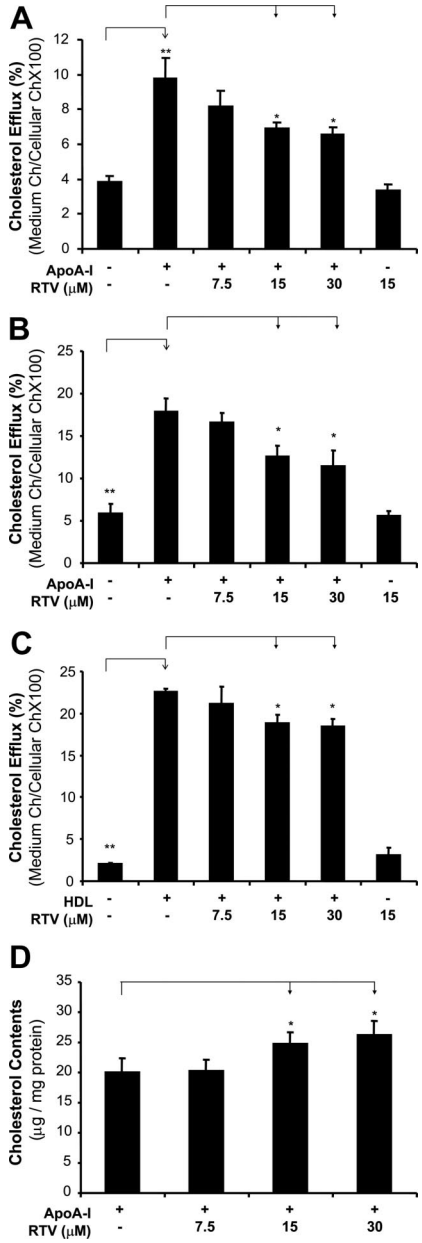

Figure 1. Effect of ritonavir on cholesterol efflux in macrophage-derived foam cells. Macrophages were transformed into foam cells by incubation with acLDL and [1α,2α(n)-^{3}H]cholesterol for 48 hours. The medium containing radioactive isotope was then removed. The cells were incubated for 24 hours in the presence or absence of ritonavir (7.5, 15, and 30 μmol/L), followed by the addition of apoA-I (50 μg/ml) or HDL (100 μg/ml) for 24 hours to initiate cholesterol efflux. Radioactivity of both medium and cellular fractions was measured, and the cholesterol efflux was calculated as [cpm-(medium)/cpm(medium + cells)] × 100%. **A** and **C:** Cholesterol efflux in THP-1 to apoA-I (**A**) or HDL (**C**) was inhibited by ritonavir in a concentration-dependent manner as compared with controls, which were cells with apoA-I or HDL only. **B:** Cholesterol efflux in PBMCs to apoA-I was inhibited by ritonavir in a concentration-dependent manner, as compared with controls. **D:** Cellular cholesterol levels were measured with a cholesterol assay kit. Accumulation of cholesterol was increased in ritonavir-treated THP-1 cells as compared with controls. Data represent mean ± SEM. $^*P < 0.05$, $^{**}P < 0.001$ versus controls, $n = 6$. PBMCs, peripheral blood mononuclear cells.

addition of apoA-I (50 μg/ml) or HDL (100 μg/ml). In both THP-1 and PBMCs, significant decreases of cholesterol efflux to apoA-I were observed in a concentration-dependent manner in response to ritonavir treatment (Figure 1, A and B). At 15 μmol/L ritonavir, the cholesterol efflux from THP-1 and PBMCs showed a significant decrease by 30 and 29%, respectively, as compared with controls (apoA-I only) ($P < 0.05$ for both, $n = 6$). Meanwhile, another cholesterol acceptor, HDL, was also used to evaluate the effect of ritonavir on the cholesterol efflux in THP-1. Consistently with apoA-I, ritonavir treatment also induced a significant decrease of cholesterol efflux from foam cells to HDL in a concentration-dependent manner (Figure 1C). The cholesterol efflux from THP-1 treated with 15 μmol/L ritonavir was significantly decreased by 17% compared with controls (HDL only) ($P = 0.01$, $n = 6$). Moreover, cellular cholesterol levels in ritonavir-treated foam cells were directly measured by an enzymatic colorimetric method. The cellular cholesterol levels in the foam cells treated with 15 μmol/L ritonavir were significantly increased by 28% compared with controls (apoA-I only) ($P = 0.04$, $n = 6$; Figure 1D).

Ritonavir Decreases the Expression of SR-B1 and Caveolin-1 in Macrophage-Derived Foam Cells

To determine whether ritonavir could affect several key molecules involved in cholesterol efflux, the expression of SR-B1, caveolin-1, caveolin-2, ABCA1, and CYP27A1 in foam cells treated by ritonavir was analyzed with real-time RT-PCR and Western blot. Treatment with ritonavir decreased the mRNA and protein levels of SR-B1 and caveolin-1 in foam cells in a concentration-dependent manner (Figure 2). At 15 and 30 μmol/L ritonavir, SR-B1 mRNA was significantly reduced by 13 and 22%, respectively, and caveolin-1 mRNA was significantly decreased by 27 and 28%, respectively, compared with controls (Figure 2, A and B; $n = 4$; $P < 0.05$). Consistently with mRNA data, protein levels of SR-B1 and caveolin-1 were also significantly reduced in ritonavir-treated cells (Figure 2, C and D). However, the mRNA and protein levels of ABCA1 (Figure 3, A, C, and D), ABCG1 (Figure 3, B, C, and E), CYP27A1, and caveolin-2 did not show any significant changes between the ritonavir-treated groups and controls (data not shown).

Ritonavir Increases Superoxide Anion Production in Macrophage-Derived Foam Cells

To investigate whether oxidative stress could be involved in the ritonavir-induced decrease of cholesterol efflux, superoxide anion production from macrophage-derived foam cells was analyzed by flow cytometric measurement of DHE staining. DHE is freely permeable to cells and is readily oxidized by superoxide anion to form ethidium bromide, which intercalates with the DNA (red fluorescence). Thus, DHE staining detected by flow cytometry (detecting red fluorescence intensity) indicates the cellular production levels of superoxide anion. Foam cells treated with 15 μmol/L ritonavir for 24 hours revealed a significant increase of superoxide anion production by 117% as compared with controls (Figure 4, A and B; $P < 0.05$). The addition of 50 μmol/L SeMet, an antioxidant, significantly inhibited ritonavir-enhanced superoxide anion production by 43% (Figure 4, A and B; $P < 0.05$). Furthermore, 50 μmol/L SeMet and 10 μmol/L ginsenoside Rb1 significantly increased cholesterol efflux from foam cells to apoA-I by 20 and 21%, respectively, as compared with treatment of 15 μmol/L ritonavir alone group (Figure 4C, $P < 0.05$). Thus, these data demonstrate that oxidative stress (increase of superoxide anion production) is involved in the mechanism of ritonavir-inhibition of cholesterol efflux in THP-1 derived form cells.

Ritonavir Decreases Mitochondrial Membrane Potential and ATP Production in Macrophage-Derived Foam Cells

To determine whether the mitochondria could be a possible source of ritonavir-induced superoxide anion production, the mitochondrial functions of membrane potential and ATP production were analyzed. Mitochondrial dysfunction could result in the increase of superoxide anion production and the decrease of ATP production. Macrophage-derived foam cells treated with 15 μmol/L ritonavir for 24 hours revealed a substantial reduction of mitochondrial membrane potential by 50% compared with controls (Figure 5, A and B; $P < 0.05$). Furthermore, treatment of 15 μmol/L ritonavir significantly reduced ATP levels by 24% compared with controls (Figure 5C, $P < 0.01$).

Ritonavir Increases mRNA Levels of NADH/NADPH Oxidase Subunits in Macrophage-Derived Foam Cells

To test whether internal molecules related to ROS could play a role in ritonavir-induced oxidative stress, we determined mRNA levels of NADH/NADPH oxidase subunits, major ROS-generating enzymes, and several major internal antioxidant enzymes such as superoxide dismutases, catalase, and glutathione peroxidase.[22,23] Oxidative stress could result from up-regulation of ROS-generating enzymes and/or down-regulation of internal antioxidant enzymes. Treatment with ritonavir significantly increased mRNA levels of NADPH oxidase subunits $p22^{phox}$, $p40^{phox}$, $p47^{phox}$, and $p67^{phox}$ in foam cells in a concentration-dependent manner (Figure 5D, $P < 0.05$). However, the expression of catalase, glutathione peroxidase-1, and superoxide dismutase-1 did not show any significant changes between the ritonavir-treated groups and controls (data not shown).

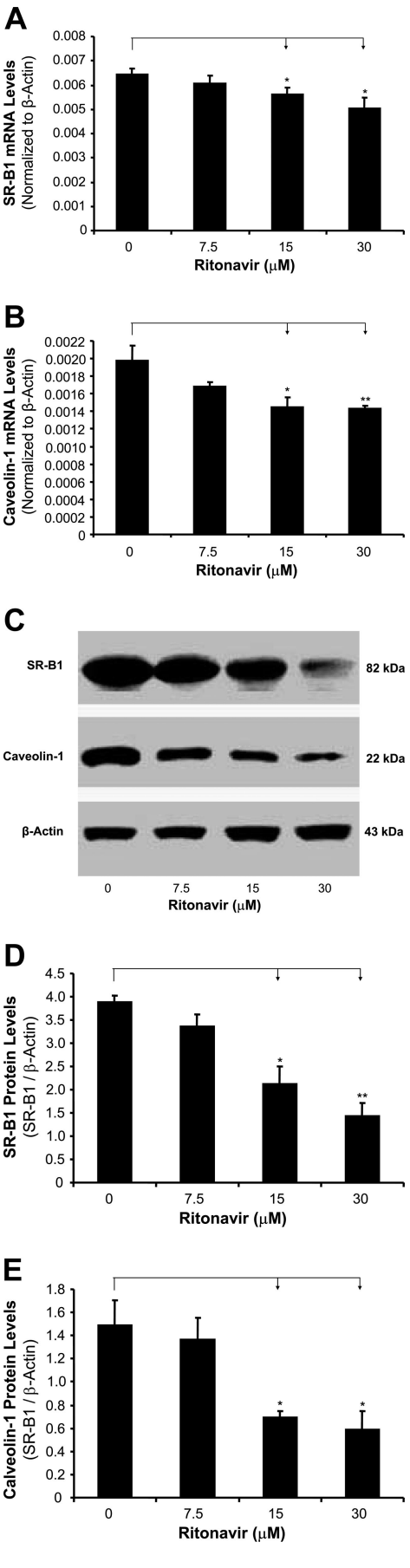

ERK1/2 Activation Is Involved in the Ritonavir-Induced Inhibition of Cholesterol Efflux in Macrophage-Derived Foam Cells

To determine whether MAPKs could be involved in signal transduction pathways of ritonavir-induced inhibition of cholesterol efflux from macrophage-derived foam cells, the activation status of three major MAPKs (ERK1/2, JNK, and p38) was determined by a Bio-Plex immunoassay with Luminex technology. Ritonavir treatment (15 μmol/L) for 60 minutes substantially increased the phosphorylation of ERK1/2 in macrophage-derived foam cells by 3.2-fold compared with controls (Figure 6A). However, there were no substantial changes in phosphorylation of JNK and P38 MAPKs in response to ritonavir treatment (data not shown). Furthermore, the specific ERK1/2 inhibitor PD98059 (20 μmol/L) significantly abolished ritonavir-induced inhibition of cholesterol efflux from macrophage-derived foam cells by 42% when compared with the treatment of ritonavir (Figure 6B, $P < 0.05$).

The involvement of the ERK1/2 pathway in cholesterol efflux in ritonavir-treated THP-1 cells was also tested with infection of a recombinant adenovirus encoding the dominant-negative form of ERK2. Another recombinant adenovirus encoding GFP was used as a control. Figure 6C shows that the cells infected by recombinant adenovirus encoding dominant-negative form of ERK2 had a dramatic increase in ritonavir-induced decreased cholesterol efflux compared with cells infected with GFP control virus ($P = 0.03$, $n = 6$). These data indicate that suppressing ERK activation by dominant-negative form of ERK2 effectively blocks the inhibition of cholesterol efflux induced by ritonavir.

Discussion

Clinical data suggest that HIV PIs may be associated with a high risk of accelerated atherosclerosis,[24] and current data provide possible mechanisms for this complication. Based on our knowledge, the present study, for the first time, reports three novel findings: 1) ritonavir inhibits cholesterol efflux from human macrophage-derived foam cells; 2) ritonavir decreases expression levels of SR-B1 and caveolin-1, which are key molecules mediating cholesterol efflux; and 3) ritonavir increases superoxide anion production and activates ERK1/2, which may function as signal transduction pathways for ritonavir's action in macrophage-derived foam cells. The inhibition of cholesterol efflux from human macrophage-derived foam cells

Figure 2. Effect of ritonavir on the expression of SR-B1 and caveolin-1 in macrophage-derived foam cells. Foam cells were treated with ritonavir (7.5, 15, and 30 μmol/L) for 24 hours. The mRNA levels of SR-B1 and caveolin-1 were measured by real-time PCR. The mRNA level of each gene in each sample was normalized to that of β-actin. Relative mRNA levels were presented as $2^{[Ct(\beta\text{-actin}) - Ct(\text{gene of interest})]}$. Ritonavir significantly decreased the mRNA levels of SR-B1 (**A**) and caveolin-1 (**B**) in a concentration-dependent manner. The protein levels of SR-B1 and caveolin-1 were measured by Western blot (**C**). Densitometric analysis was performed to quantify the relative expression of proteins. Ritonavir significantly decreased the protein levels of SR-B1 (**D**) and caveolin-1 (**E**) in a concentration-dependent manner. Data represent mean ± SEM. $^*P < 0.05$, $^{**}P < 0.01$ versus controls, $n = 4$.

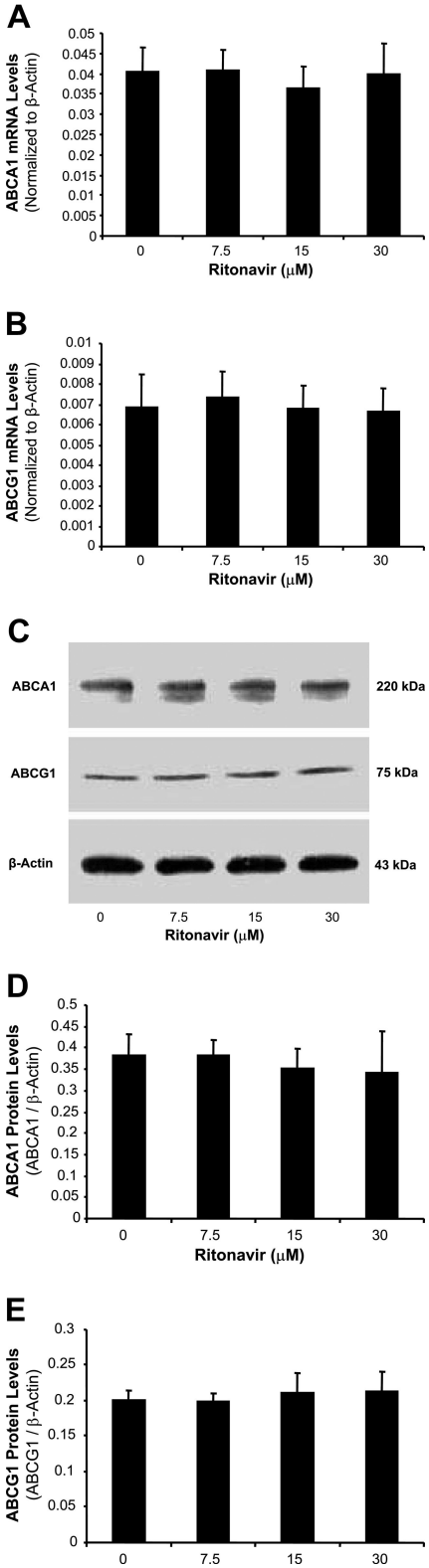

Figure 3. Effect of ritonavir on the expression of ABCA1 and ABCG1 in macrophage-derived foam cells. Foam cells were treated with ritonavir (7.5, 15, and 30 μmol/L) for 24 hours. The mRNA levels of ABCA1 (**A**) and ABCG1 (**B**) were measured by real-time PCR. **C:** The protein levels of ABCA1 and ABCG1 were measured by Western blot. **D** and **E:** Densitometric analysis was performed to quantify the relative expression of proteins. The mRNA and protein levels of ABCA1 and ABCG1 did not show any significant changes between the ritonavir-treated groups and controls. Data represent mean ± SEM, $n = 4$.

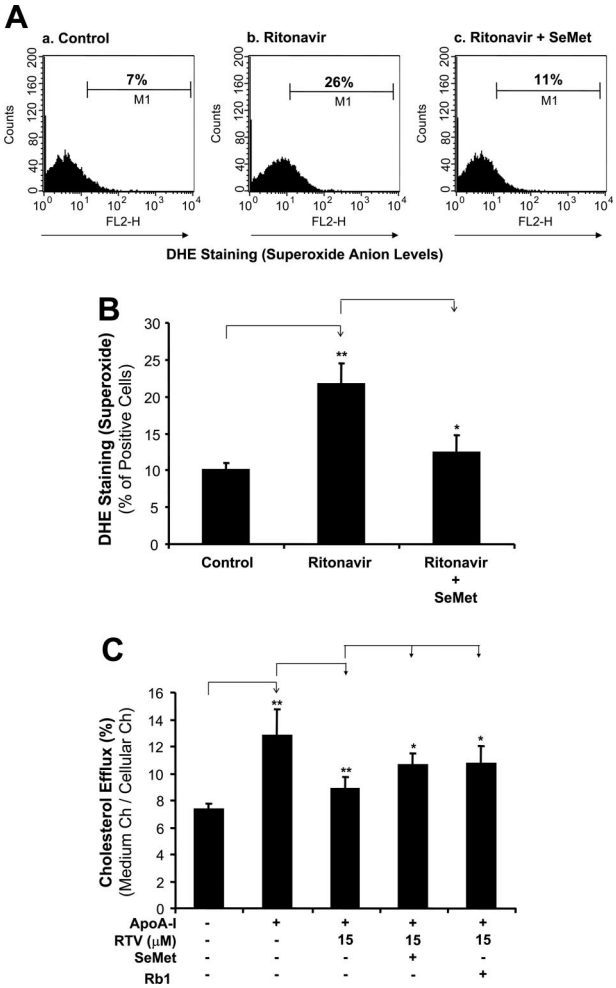

Figure 4. Effects of ritonavir and SeMet on superoxide anion production and cholesterol efflux in macrophage-derived foam cells. Foam cells were treated with 15 μmol/L ritonavir in the presence or absence of 50 μmol/L SeMet. **A:** Superoxide anion in the cells was analyzed by flow cytometric analysis of DHE staining. **a:** Untreated foam cells with DHE staining served as a staining control. **b:** Cells were treated with ritonavir. **c:** Cells were treated with ritonavir and SeMet simultaneously. **B:** Results from three separate experiments were averaged, showing that ritonavir increased superoxide anion production and SeMet significantly inhibited the ritonavir-induced increase of superoxide anion production in macrophage-derived foam cells. $n = 3$. **C:** In separate experiments, foam cells were treated with 15 μmol/L ritonavir in the presence or absence of 50 μmol/L SeMet or 10 μmol/L ginsenoside Rb1 for 24 hours, followed by an addition of apoA-I (50 μg/ml) for 24 hours to initiate cholesterol efflux. Both SeMet and ginsenoside Rb1 significantly inhibited the ritonavir-induced decrease of cholesterol efflux in macrophage-derived foam cells. Data represent mean ± SEM. $^*P < 0.05$ versus ritonavir-treated group, $^{**}P < 0.001$ versus controls, $n = 6$.

by ritonavir could contribute to the accumulation of cholesterol in the foam cell, thereby attributing to the progression of atherosclerosis on the arterial wall.

Ritonavir was selected for the current study because it is one of the most commonly used HIV PIs as part of highly active anti-retroviral therapy. Recommended clinical dose of ritonavir is 600 mg every 12 hours resulting in a maximum plasma concentration of 8 to 15 μmol/L. The concentration (15 μmol/L) of ritonavir used in the present study may be relevant to its clinical application.[25] Our data show that 15 μmol/L ritonavir significantly reduced cholesterol efflux in THP-1-derived foam cells by 30% as compared with controls. Increased accumulation of intra-

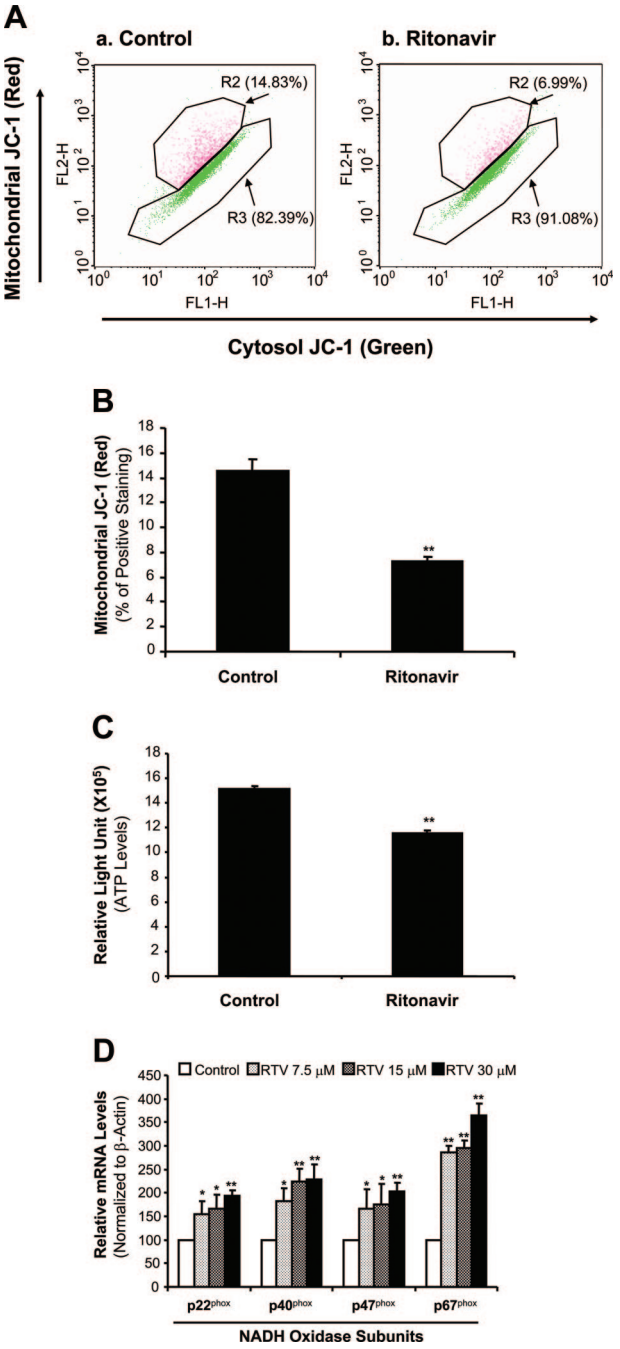

Figure 5. Effects of ritonavir on mitochondrial membrane potential, ATP production, and the mRNA levels of NADPH oxidase subunits in macrophage-derived foam cells. Microphage-derived foam cells were treated with 15 μmol/L ritonavir for 24 hours. **A** and **B:** Mitochondrial membrane potential ($\Delta\psi$m) was determined with JC-1 staining and flow cytometry analysis. Ritonavir significantly decreased the mitochondrial membrane potential (red) in THP-1 cells compared with controls. $n = 3$. **C:** Cellular ATP levels were measured with an ATPLite kit. ATP production was significantly reduced in ritonavir-treated THP-1 cells compared with controls. $n = 6$. **D:** The mRNA levels of NADPH oxidase subunits were measured by real-time PCR. Ritonavir significantly increased the mRNA levels of $p22^{phox}$, $p40^{phox}$, $p47^{phox}$, and $p67^{phox}$ in a concentration-dependent manner. Data represent mean ± SEM. $^{*}P < 0.05$, $^{**}P < 0.01$ versus controls (without ritonavir). $n = 4$.

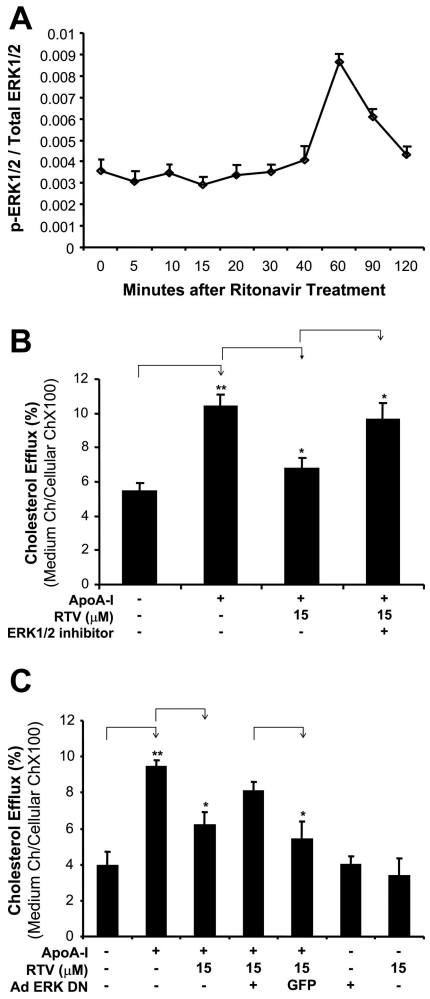

Figure 6. Role of ERK1/2 in ritonavir-induced inhibitor of cholesterol efflux in macrophage-derived foam cells. **A:** Effect of ritonavir on ERK1/2 activation. Macrophage-derived foam cells were treated with 15 μmol/L ritonavir for different durations. The phosphorylated and total ERK proteins were detected by the Bio-Plex immunoassay system. Ritonavir treatment increased the ratio of phosphorylated and total ERK1/2 protein at 60 minutes after treatment. $n = 2$. **B:** Effect of ERK1/2 inhibitor on ritonavir-induced inhibition of cholesterol efflux. Macrophage-derived foam cells were treated with 15 μmol/L ritonavir with or without 20 μmol/L PD98059, an inhibitor of ERK1/2, for 24 hours, followed by the addition of apoA-I (50 μg/ml) for 24 hours to initiate cholesterol efflux. Cholesterol efflux was inhibited by ritonavir, and pretreatment of ERK1/2 inhibitor significantly abolished the inhibition of cholesterol efflux from macrophage-derived foam cells to apoA-I. **C:** Effect of dominant-negative mutant of ERK2 gene delivery on ritonavir-induced inhibition of cholesterol efflux. THP-1 cells were infected with a recombinant adenovirus encoding dominant-negative form of ERK2. Another recombinant adenovirus encoding GFP was used as a control. Infected cells were treated with 15 μmol/L ritonavir, followed by the addition of apoA-I (50 μg/ml) for 24 hours to initiate cholesterol efflux. Overexpression of dominant-negative form of ERK2 effectively blocked ritonavir-induced decreased cholesterol efflux as compared with GFP controls. Data represent mean ± SEM. $^{*}P < 0.05$ versus ritonavir-treated group or infected with GFP group. $^{**}P < 0.001$ versus controls, $n = 6$.

cellular cholesterol in the ritonavir-treated foam cells was also demonstrated by direct measurement. Dressman and colleagues[13] reported that ritonavir could increase the level of cholesterol ester, which is a CD36-dependent cholesterol accumulation, in THP-1 macrophages and human PBMCs. However, it is not clear that the accumulation of cholesterol in macrophages is attributable to the increased influx or the decreased efflux of cholesterol. The present study further illustrates that the inhibition of cholesterol efflux by ritonavir treatment may be attributable to the accumulation of cholesterol in macro-

phages, which most likely promote the progression of atherosclerosis.

Because cholesterol acceptors such as apoA-I and HDL approach macrophages in subintimal space, intracellular cholesterol can be released outside the cells for excretion. In this pathway, several key molecules including SR-B1, caveolins, ABCA1, ABCG1, and CYP27A1 have been known to mediate cholesterol efflux.[6–10] Expression of SR-B1 correlates with rates of cholesterol efflux to HDL.[8] Down-regulation of caveolin-1 by treatment with anti-sense oligonucleotides was reported to decrease cholesterol efflux to apoA-I.[9] However, it has not been definitively established what acceptors are dependent on the changes of special proteins during the cholesterol efflux in the various types of cells. For example, in addition to apoA-I, several of the other exchangeable apolipoproteins including apoA-II, apoC-II, apoC-III, and apoE have been shown to stimulate ABCA1-mediated lipid efflux.[26] Palmer and colleagues[20] reported that triglyceride-rich lipoprotein, an independent risk factor for coronary artery disease, could inhibit cholesterol efflux in THP-1-derived macrophages to apoA-I, whereas it did not affect levels of ABCA1, SR-B1, and caveolin-1, suggesting that exposure to these lipoproteins inhibits an alternate anti-atherogenic pathway. The present study shows that treatment with ritonavir could inhibit cholesterol efflux from macrophages to either apoA-I or HDL, which is accompanied with a decreased expression of SR-B1 and caveolin-1 but not ABCA1, ABCG1, caveolin-2, and CYO27A1, in foam cells. These data indicate that down-regulation of SR-B1 and caveolin-1 may be involved in the inhibition of cholesterol efflux in ritonavir-treated macrophages.

Decreases of SR-B1 and caveolin-1 could have functional significance in cholesterol efflux. SR-B1 shows a partial co-localization with caveolin-1 by immunofluorescence, indicating the close relationship between caveolin-1 and SR-B1.[27] A study reported a modest (30 to 40%) inhibition of SR-BI-dependent selective uptake of cholesterol in the caveolin-1-overexpressing line (human embryonic kidney 293).[28] However, a study from Wang and colleagues[29] shows that SR-BI-stimulated cholesterol efflux to HDL and liposomes and SR-B1-mediated selective uptake of HDL-derived cholesteryl ester are not affected by caveolin-1 expression in human embryonic kidney 293 or FRT cells.

Although SR-B1 and carevolin-1 at both mRNA and protein levels are significantly reduced in the ritonavir-treated cells as compared with control cells, the decrease of their mRNA levels in the ritonavir-treated cells is relatively smaller than that of their protein levels. The reasons for this discrepancy are not clear. It could be involved in different processes of the translation from mRNA to protein and the turnover rate of both mRNA and proteins. It could also be affected by the sensitivity of detection methods and sample sizes. Real-time PCR and Western blot may have different sensitivity for quantitative measurements.

ROS, generated by a variety of extracellular and intracellular mechanisms, have gained attention as novel signal mediators that regulate signal transduction events including MAPKs. ROS includes superoxide anion, hydroxyl radical, nitric oxide, peroxynitrite, and lipid radicals. Accumulating evidence suggests that an increase in ROS generation may relate to a risk for cardiovascular diseases such as atherosclerosis, angina pectoris, and myocardial infarction. Antioxidants are believed to counteract with ROS and reduce the incidence of coronary artery disease.[30] Ritonavir is known to induce ROS in endothelial cells and vascular smooth muscle cells.[14–17] However, little is known about the potency of ritonavir to induce macrophage ROS production as well as the role of ROS in the ritonavir-induced inhibition of cholesterol efflux in foam cells. The present study demonstrates that ritonavir at the concentration equivalent to the therapeutic levels is able to increase superoxide anion production in human macrophage-derived foam cells. This effect is specific because an antioxidant compound, either SeMet or ginsenoside Rb1, is able to block the ritonavir-induced increase of superoxide anion production as well as ritonavir-induced inhibition of cholesterol efflux in macrophage-derived foam cells. SeMet and ginsenoside Rb1 were selected in the current study because of their low toxicity, and readiness for animal or human use. Findings from the current study suggest that ritonavir-induced oxidative stress may be one of the molecular mechanisms involved in the inhibition of cholesterol efflux. Accordingly, the use of antioxidants may be an effective strategy in preventing ritonavir-associated cardiovascular complications in HIV patients.

It is well known that the mitochondrion is one of the major sources of ROS generation.[31] After oxidation by mitochondrial and plasma membrane oxidases, oxygen is reduced and the superoxide anion is formed. The membrane potential ($\Delta\psi m$) can serve as an indicator for the function of mitochondrial respiration chain. Mitochondrial dysfunction could cause the increase of superoxide anion production and the decrease of ATP production. The purpose of the mitochondrial experiment in the current study was to determine whether mitochondria could be a possible source of the increased superoxide anion production in ritonavir-treated cells. Indeed, our data support this hypothesis that mitochondrial dysfunction could cause the increase of superoxide anion production in ritonavir-treated cells. The mitochondrial dysfunction could be critical part of the molecular pathway of the inhibition of cholesterol efflux in ritonavir-treated cells.

Other important sources of ROS within cells include the synthesis by dedicated enzymes including NADPH oxidase, which is best characterized as a major superoxide-generating enzyme in phagocytes. NADPH oxidase is a multicomponent enzyme comprised of five subunits, namely $p22^{phox}$, $p40^{phox}$, $p47^{phox}$, $p67^{phox}$, and $gp91^{phox}$.[30] Our previous study has indicated that ritonavir also increased NADPH oxidase activity in porcine arteries.[17] Consistently with our previous data, treatment with ritonavir increased the expression of $p22^{phox}$, $p40^{phox}$, $p47^{phox}$, and $p67^{phox}$ in foam cells. Thus, these data indicate that increased superoxide anion production in ritonavir-treated foam cells may result from mitochondrial dysfunction and up-regulation of NADPH oxidase.

ROS including superoxide anion could play important roles in both signal transduction pathways and cell damage. In the current study, ritonavir could increase production of superoxide anion, decrease the expression of SR-B1 and caveolin-1, and inhibit cholesterol efflux in human macrophages. However, it is not clear whether superoxide anion directly regulates the expression of SR-B1 and/or caveolin-1 expression. In some other reports, lipopolysaccharide (LPS) could induce oxidative stress, decrease SR-B1 expression, and inhibit cholesterol efflux in mouse macrophages (RAW cells).[32] Endothelin-1 could also enhance oxidative stress and downregulate caveolin-1 expression in human endothelial cells.[33] However, Peterson and colleagues[34] reported that there were no significant changes in caveolin-1 expression in cultured bovine aortic endothelial cells in response to any treatment of ROS (using LY83583 to generate superoxide). It is well documented that ERK1/2 is an oxidation-sensitive enzyme.[35] In the current study, increased production of superoxide anion could be directly involved in ERK1/2 activation, which may regulate cholesterol efflux in human macrophages, because both antioxidant SeMet and ERK1/2 inhibitors can effectively block the ritonavir-induced inhibition of cholesterol efflux. Thus, ritonavir-induced oxidative stress could play a central role in the regulation of cholesterol efflux in human macrophages.

Cholesterol efflux from macrophages is a complicated biological process that involves many functional and regulatory molecules including signal transduction pathways. For examples, the activation of Rho family G proteins (ie, Cdc42, Rac1, and Rho) and stress kinases (ie, JNK and p38 MAPK) and activation of Cdc42 and JNK is involved in the apoA-I-induced cholesterol efflux.[36] The exposure of human fibroblasts to ABCA1 ligands results in the generation of intracellular signals, including activation of the small G-protein Cdc42, protein kinases (PAK-1 and p54JNK), and actin polymerization.[37] It was reported that cAMP-mediated cholesterol efflux to apoA-I is associated with the binding, uptake, and resecretion of apoA-I in a calcium-dependent pathway in murine macrophages. cAMP/protein kinase A (PKA)-dependent pathway modulates cellular lipid efflux mediated by apoA-I in fibroblasts.[38,39]

The current study clearly demonstrates that ERK1/2 activation is involved in the inhibition of cholesterol efflux in ritonavir-treated cells. ERK1/2 phosphorylation levels are substantially increased by ritonavir treatment, and specific inhibitor of ERK1/2 could also effectively block the inhibition of cholesterol efflux in ritonavir-treated macrophage-derived foam cells. This mechanism is consistent with some other activators of ERK1/2 such as tumor necrosis factor-α, interleukin-1, and endotoxin, which could activate ERK1/2 and inhibit cholesterol efflux in macrophages.[40–42]

In summary, the present study demonstrates that the interaction of ritonavir with cholesterol-loaded macrophages decreases the cholesterol efflux as well as downregulates the levels of SR-B1 and caveolin1 in these cells. Accumulation of cholesterol in macrophages resulting from inhibition of cholesterol efflux could be one of the important factors attributing to the progression of atherosclerosis. This study demonstrates a clear link between HIV PI ritonavir and *in vitro* cholesterol efflux, for which the increase of oxidative stress and activation of ERK1/2 may be the molecular mechanism. Consequently, reducing oxidative stress or inhibiting ERK1/2 activation may be able to shed new light on prevention of ritonavir-associated cardiovascular complications.

References

1. Navia MA, Fitzgerald PM, McKeever BM, Leu CT, Heimbach JC, Herber WK, Sigal IS, Darke PL, Springer JP: Three-dimensional structure of aspartyl protease from human immunodeficiency virus HIV-1. Nature 1989, 337:615–620
2. Shankar SS, Dube MP: Clinical aspects of endothelial dysfunction associated with human immunodeficiency virus infection and antiretroviral agents. Cardiovasc Toxicol 2004, 4:261–269
3. Palella Jr FJ, Delaney KM, Moorman AC, Loveless MO, Fuhrer J, Satten GA, Aschman DJ, Holmberg SD: Declining morbidity and mortality among patients with advanced human immunodeficiency virus infection. HIV Outpatient Study Investigators. N Engl J Med 1998, 338:853–860
4. Sviridov D, Nestel P: Dynamics of reverse cholesterol transport: protection against atherosclerosis. Atherosclerosis 2002, 161:245–254
5. Ohashi R, Mu H, Wang X, Yao Q, Chen C: Reverse cholesterol transport and cholesterol efflux in atherosclerosis. QJM 2005, 98:845–856
6. Klucken J, Buchler C, Orso E, Kaminski WE, Porsch-Ozcurumez M, Liebisch G, Kapinsky M, Diederich W, Drobnik W, Dean M, Allikmets R, Schmitz G: ABCG1 (ABC8), the human homolog of the Drosophila white gene, is a regulator of macrophage cholesterol and phospholipid transport. Proc Natl Acad Sci USA 2000, 97:817–822
7. Bodzioch M, Orso E, Klucken J, Langmann T, Bottcher A, Diederich W, Drobnik W, Barlage S, Buchler C, Porsch-Ozcurumez M, Kaminski WE, Hahmann HW, Oette K, Rothe G, Aslanidis C, Lackner KJ, Schmitz G: The gene encoding ATP-binding cassette transporter 1 is mutated in Tangier disease. Nat Genet 1999, 22:347–351
8. de La Llera-Moya M, Connelly MA, Drazul D, Klein SM, Favari E, Yancey PG, Williams DL, Rothblat GH: Scavenger receptor class B type I affects cholesterol homeostasis by magnifying cholesterol flux between cells and HDL. J Lipid Res 2001, 42:1969–1978
9. Arakawa R, Abe-Dohmae S, Asai M, Ito JI, Yokoyama S: Involvement of caveolin-1 in cholesterol enrichment of high density lipoprotein during its assembly by apolipoprotein and THP-1 cells. J Lipid Res 2000, 41:1952–1962
10. Escher G, Krozowski Z, Croft KD, Sviridov D: Expression of sterol 27-hydroxylase (CYP27A1) enhances cholesterol efflux. J Biol Chem 2003, 278:11015–11019
11. Gesquière L, Loreau N, Minnich A, Davignon J, Blache D: Oxidative stress leads to cholesterol accumulation in vascular smooth muscle cells. Free Radic Biol Med 1999, 27:134–145
12. Ross R: The pathogenesis of atherosclerosis: a perspective for the 1990s. Nature 1993, 362:801–809
13. Dressman J, Kincer J, Matveev SV, Guo L, Greenberg RN, Guerin T, Meade D, Li XA, Zhu W, Uittenbogaard A, Wilson ME, Smart EJ: HIV protease inhibitors promote atherosclerotic lesion formation independent of dyslipidemia by increasing CD36-dependent cholesteryl ester accumulation in macrophages. J Clin Invest 2003, 111:389–397
14. Chai H, Zhou W, Lin P, Lumsden A, Yao Q, Chen C: Ginsenosides block HIV protease inhibitor ritonavir-induced vascular dysfunction of porcine coronary arteries. Am J Physiol 2005, 288:H2965–H2971
15. Chai H, Yan S, Lin P, Lumsden AB, Yao Q, Chen C: Curcumin blocks HIV protease inhibitor ritonavir-induced vascular dysfunction in porcine coronary arteries. J Am Coll Surg 2005, 200:820–830
16. Chen C, Lu XH, Yan S, Chai H, Yao Q: HIV protease inhibitor ritonavir increases endothelial monolayer permeability. Biochem Biophys Res Commun 2005, 335:874–382
17. Conklin BS, Fu W, Lin PH, Lumsden AB, Yao Q, Chen C: HIV protease inhibitor ritonavir decreases endothelium-dependent vasorelaxation

and increases superoxide in porcine arteries. Cardiovasc Res 2004, 63:168–175
18. Fu W, Chai H, Yao Q, Chen C: Effects of HIV protease inhibitor ritonavir on vasomotor function and endothelial nitric oxide synthase expression. J Acquir Immune Defic Syndr 2005, 39:152–158
19. Stein JH, Klein MA, Bellehumeur JL, McBride PE, Wiebe DA, Otvos JD, Sosman JM: Use of human immunodeficiency virus-1 protease inhibitors is associated with atherogenic lipoprotein changes and endothelial dysfunction. Circulation 2001, 104:257–262
20. Palmer AM, Murphy N, Graham A: Triglyceride-rich lipoproteins inhibit cholesterol efflux to apolipoprotein (apo) A1 from human macrophage foam cells. Atherosclerosis 2004, 173:27–38
21. Wang X, LeMaire SA, Chen L, Shen Y, Gan Y, Utama B, Ou H, Bartsch H, Carter S, Coselli J, Wang XL: Increased collagen deposition and elevated expression of connective tissue growth factor in human thoracic aortic dissection. Circulation 2006, 114:I200–I205
22. Matés JM, Perez-Gomez C, Nunez de Castro I: Antioxidant enzymes and human diseases. Clin Biochem 1999, 32:595–603
23. Matés JM, Sanchez-Jimenez F: Antioxidant enzymes and their implications in pathophysiologic processes. Front Biosci 1999, 4:D339–D345
24. Maggi P, Serio G, Epifani G, Fiorentino G, Saracino A, Fico C, Perilli F, Lillo A, Ferraro S, Gargiulo M, Chirianni A, Angarano G, Regina G, Pastore G: Premature lesions of the carotid vessels in HIV-1-infected patients treated with protease inhibitors. AIDS 2000, 14:F123–F128
25. Deeks SG, Smith M, Holodniy M, Kahn JO: HIV-1 protease inhibitors. A review for clinicians. JAMA 1997, 277:145–153
26. Remaley AT, Stonik JA, Demosky SJ, Neufeld EB, Bocharov AV, Vishnyakova TG, Eggerman TL, Patterson AP, Duverger NJ, Santamarina-Fojo S, Brewer Jr HB: Apolipoprotein specificity for lipid efflux by the human ABCAI transporter. Biochem Biophys Res Commun 2001, 280:818–823
27. Babitt J, Trigatti B, Rigotti A, Smart EJ, Anderson RG, Xu S, Krieger M: Murine SR-BI, a high density lipoprotein receptor that mediates selective lipid uptake, is N-glycosylated and fatty acylated and colocalizes with plasma membrane caveolae. J Biol Chem 1997, 272:13242–13249
28. Frank PG, Marcel YL, Connelly MA, Lublin DM, Franklin V, Williams DL, Lisanti MP: Stabilization of caveolin-1 by cellular cholesterol and scavenger receptor class B type I. Biochemistry 2002, 41:11931–11940
29. Wang L, Connelly MA, Ostermeyer AG, Chen HH, Williams DL, Brown DA: Caveolin-1 does not affect SR-BI-mediated cholesterol efflux or selective uptake of cholesteryl ester in two cell lines. J Lipid Res 2003, 44:807–815
30. Rimm EB, Stampfer MJ, Ascherio A, Giovannucci E, Colditz GA, Willett WC: Vitamin E consumption and the risk of coronary heart disease in men. N Engl J Med 1993, 328:1450–1456
31. Genova ML, Pich MM, Bernacchia A, Bianchi C, Biondi A, Bovina C, Falasca AI, Formiggini G, Castelli GP, Lenaz G: The mitochondrial production of reactive oxygen species in relation to aging and pathology. Ann NY Acad Sci 2004, 1011:86–100
32. Baranova I, Vishnyakova T, Bocharov A, Chen Z, Remaley AT, Stonik J, Eggerman TL, Patterson AP: Lipopolysaccharide down regulates both scavenger receptor B1 and ATP binding cassette transporter A1 in RAW cells. Infect Immun 2002, 70:2995–3003
33. Dong F, Zhang X, Wold LE, Ren Q, Zhang Z, Ren J: Endothelin-1 enhances oxidative stress, cell proliferation and reduces apoptosis in human umbilical vein endothelial cells: role of ETB receptor, NADPH oxidase and caveolin-1. Br J Pharmacol 2005, 145:323–333
34. Peterson TE, Poppa V, Ueba H, Wu A, Yan C, Berk BC: Opposing effects of reactive oxygen species and cholesterol on endothelial nitric oxide synthase and endothelial cell caveolae. Circ Res 1999, 85:29–37
35. Baas AS, Berk BC: Differential activation of mitogen-activated protein kinases by H_2O_2 and O_2^- in vascular smooth muscle cells. Circ Res 1995, 77:29–36
36. Nofer JR, Remaley AT, Feuerborn R, Wolinnska I, Engel T, von Eckardstein A, Assmann G: Apolipoprotein A-I activates Cdc42 signaling through the ABCA1 transporter. J Lipid Res 2006, 47:794–803
37. Nofer JR, Feuerborn R, Levkau B, Sokoll A, Seedorf U, Assmann G: Involvement of Cdc42 signaling in apoA-I-induced cholesterol efflux. J Biol Chem 2003, 278:53055–53062
38. Fitzgerald ML, Morris AL, Chroni A, Mendez AJ, Zannis VI, Freeman MW: ABCA1 and amphipathic apolipoproteins form high-affinity molecular complexes required for cholesterol efflux. J Lipid Res 2004, 45:287–294
39. Haidar B, Denis M, Krimbou L, Marcil M, Genest Jr J: cAMP induces ABCA1 phosphorylation activity and promotes cholesterol efflux from fibroblasts. J Lipid Res 2002, 43:2087–2094
40. Khovidhunkit W, Moser AH, Shigenaga JK, Grunfeld C, Feingold KR: Endotoxin down-regulates ABCG5 and ABCG8 in mouse liver and ABCA1 and ABCG1 in J774 murine macrophages: differential role of LXR. J Lipid Res 2003, 44:1728–1736
41. Wajant H, Pfizenmaier K, Scheurich P: Tumor necrosis factor signaling. Cell Death Differ 2003, 10:45–65
42. Chen M, Li W, Wang N, Zhu Y, Wang X: ROS and NF-κB but not LXR mediate IL-1β signaling for the downregulation of ATP-binding cassette transporter A1. Am J Physiol Cell Physiol 2007, 292:C1493–C1501